Electronic Supplementary Material (ESI) for Dalton Transactions.

Gold setting the "gold standard" among transition metals as a hydrogen bond acceptor – a theoretical investigation

Ferdinand Groenewald, Helgard G. Raubenheimer, Jan Dillen and Catharine Esterhuysen*

Department of Chemistry and Polymer Science, University of Stellenbosch, Private Bag X1, Matieland, Stellenbosch, 7602, South Africa. E-mail: ce@sun.ac.za

Supplementary Information

S1. MP2/aug-cc-pVTZ-pp optimised coordinates

S1.1 Auride adducts

Au^-…HF

Low Frequencies

183.6831 768.3354 768.3354

Optimised Coordinates

79	0.184715	0.013922	0.019300
1	2.270255	0.013935	0.019640
9	3.248299	0.013941	0.019800

Au^-…HCN

Low Frequencies

126.0092 156.6463 156.6463

Optimised Coordinates

79	0.000000	-0.000031	0.571791
6	0.000000	-0.000031	-2.757853
1	0.000000	-0.000031	-1.638434
7	0.000000	-0.000031	-3.930035

Au^-…HCCH

Low Frequencies

96.9233 127.1568 596.6260

Optimised Coordinates

79	-0.815883	0.786665	1.668184
1	-1.106465	2.278990	-3.943945
6	-1.053513	2.006769	-2.920156
6	-0.992668	1.693943	-1.743656
1	-0.938118	1.413657	-0.689567

$Au^-\ldots H_2O$

Low Frequencies

142.1404 301.1336 669.8565

Optimised Coordinates

79	0.275048	0.007905	-0.000008
8	-2.979601	-0.090066	0.000091
1	-2.955495	0.872488	-0.000034
1	-2.004786	-0.276369	0.000089

$Au^-\ldots NH_3$

Low Frequencies

107.8151 217.2294 285.9152

Optimised Coordinates

79	0.051853	-0.118827	-0.070662
1	2.518381	0.232582	0.245212
7	3.543139	0.139095	0.181590
1	3.722648	0.183149	-0.817146
1	3.707501	-0.831859	0.430326

$Au^-\ldots CH_4$

Low Frequencies

69.3979 132.9266 132.9580

Optimised Coordinates

79	0.747751	0.052756	-0.188748
1	-3.688179	0.356377	0.211831
1	-2.077834	-0.407227	0.183937
1	-3.323872	-0.980593	1.322156
1	-3.502656	-1.294035	-0.416469
6	-3.146142	-0.581038	0.325090

S1.2 DMA adducts

DMA...HF

Low Frequencies

33.0919 39.0934 69.0696

Optimised Coordinates

79	0.460119	-0.001305	-0.089349
9	-2.190306	-0.604629	-1.724846
1	-1.430672	-0.393843	-1.188055
6	-1.069980	0.800582	1.033813
1	-1.624070	1.581867	0.500770
1	-1.801926	0.049444	1.352562
1	-0.659665	1.258268	1.942887
6	2.024900	-0.785831	-1.174069
1	2.985725	-0.616527	-0.671261
1	1.921260	-1.867991	-1.316105
1	2.098034	-0.334160	-2.170377

DMA...HCN

Low Frequencies

40.1586 44.7952 114.1498

Optimised Coordinates

79	0.571796	0.099229	-0.205159
6	-1.052396	0.934144	0.758932
1	-1.669169	1.552075	0.093486
1	-1.716523	0.180439	1.201572
1	-0.721480	1.584213	1.577756
6	2.216232	-0.710765	-1.137536
1	2.217731	-1.806248	-1.089246
1	2.265194	-0.434189	-2.197501
1	3.148150	-0.366720	-0.671684
1	-1.505841	-0.595987	-1.154484
6	-2.389765	-0.980458	-1.668164
7	-3.331054	-1.396765	-2.223703

DMA...HCCH

Low Frequencies

35.7433 38.3743 90.0012

Optimised Coordinates

79	-0.494103	-0.444217	1.217161
6	-2.109954	0.125946	2.357122
1	-2.666300	0.950991	1.895081
1	-2.819140	-0.698294	2.503350
1	-1.801075	0.465077	3.354274
6	1.140952	-1.010005	0.093716
1	2.070777	-0.885670	0.663010
1	1.094080	-2.062742	-0.213992
1	1.246242	-0.414549	-0.822520
1	-2.398411	-2.237459	-4.099673
6	-2.006601	-1.927116	-3.164257
6	-1.555076	-1.571658	-2.092158
1	-1.160078	-1.255196	-1.139413

DMA...H_2O

Low Frequencies

38.6797 50.0753 120.8610

Optimised Coordinates

79	0.457495	-0.135181	0.042064
8	-2.257853	0.055873	-1.922496
1	-2.599538	0.415579	-1.096275
1	-1.339437	-0.131106	-1.649456
6	-1.080437	0.669585	1.158008
1	-1.935035	-0.015680	1.238799
1	-0.762633	0.895812	2.183562
1	-1.452825	1.610419	0.730676
6	1.997888	-0.936066	-1.059189
1	2.913900	-1.021395	-0.460764
1	1.760030	-1.941143	-1.428312
1	2.241218	-0.320557	-1.933802

DMA...NH_3

Low Frequencies

35.0669 39.1077 60.4697

Optimised Coordinates

79	-1.130190	0.426622	-0.129015
1	1.378464	-0.228064	0.251839
7	2.284389	-0.670080	0.077494
1	2.650082	-0.186606	-0.735820
1	2.033366	-1.596417	-0.252576
6	-1.120387	-1.635323	-0.112289
1	-0.644995	-2.046793	-1.012699
1	-0.578122	-2.040128	0.752373
1	-2.136528	-2.047870	-0.071795
6	-1.144844	2.484485	-0.150158
1	-0.626362	2.907487	0.719395
1	-0.654807	2.889334	-1.044802
1	-2.168241	2.881053	-0.137988

DMA...CH_4

Low Frequencies

9.8688 31.2930 31.9996

Optimised Coordinates

79	-1.335053	-0.004985	-0.086025
6	-2.004361	-1.949380	0.020872
1	-1.644238	-2.553249	-0.822113
1	-1.668374	-2.448116	0.939209
1	-3.100748	-2.004145	0.009118
6	-0.666206	1.941731	-0.193070
1	-0.063219	2.216462	0.682506
1	-0.039134	2.111340	-1.078348
1	-1.497228	2.656889	-0.247131
6	2.666308	0.146601	-0.035144
1	1.578437	0.094216	-0.048074
1	3.042746	-0.274226	0.894962
1	2.975399	1.186526	-0.113482
1	3.070727	-0.415991	-0.874093

S1.3 Ag(I) and Cu(I) adducts

$[(Me)_2Ag]^-$...HF

Low Frequencies

19.0164 74.3421 121.6073

Optimised Coordinates

47	0.154344	0.126585	0.075657
9	-1.029039	-1.263591	-2.665216
1	-0.419577	-0.964183	-1.998342
6	-1.067828	1.063288	1.486324
1	-1.621286	1.899889	1.045382
1	-1.806147	0.368530	1.902069
1	-0.488519	1.463397	2.326543
6	1.507432	-0.785620	-1.262957
1	2.464025	-0.616289	-0.753667
1	1.417550	-1.868465	-1.401770
1	1.602461	-0.337669	-2.258050

$[(Me)_2Cu]^-$...HF

Low Frequencies

5.7437 73.8966 115.5530

Optimised Coordinates

29	0.053192	0.224685	0.238291
6	-0.907266	1.114131	1.609249
1	-1.472207	1.976572	1.229486
1	-1.637306	0.456062	2.100352
1	-0.250038	1.497354	2.402957
6	1.139976	-0.641095	-1.065989
1	2.151285	-0.519012	-0.647580
1	1.001908	-1.721150	-1.204978
1	1.175886	-0.198793	-2.069970
9	-1.548653	-1.002050	-2.235786
1	-0.881921	-0.724261	-1.614757

S1.4 Adducts with omission of relativistic effects on Au

Note that for Au the aug-cc-pVTZ-pp basis set and pseudopotential are replaced by the ECP60MHF basis set and ECP.

Au^-...HF

Low Frequencies

118.5247 595.4115 595.4116

Optimised Coordinates

79	-0.099591	0.001885	0.001450
1	2.342488	0.001852	0.000362
9	3.297461	0.001840	-0.000064

DMA...HF

Low Frequencies

5.5509 72.2363 112.2464

Optimised Coordinates

79	0.123836	0.105287	0.115525
6	-1.140439	1.121423	1.590331
1	-2.148477	1.287119	1.197918
1	-1.237266	0.533929	2.509010
1	-0.730099	2.098022	1.866816
6	1.527076	-0.907272	-1.274929
1	2.451855	-0.872734	-0.688641
1	1.339570	-1.962540	-1.496880
1	1.742213	-0.405881	-2.223788
9	-0.899761	-1.048635	-2.919107
1	-0.320076	-0.857857	-2.190255

S2. Interaction energies

Table S1 –The interaction energies (E_{INT}) in kcal/mol, intermolecular distance [*d*(Au···H)] in Å, bonding angle (Au···H-X) in degrees and the H-X distance in Å for the optimised geometries of the H-Bonded Au^- anion at four different levels of theory.

Method	H-Donor	E_{INT} (kcal/mol)	*d*(Au···H) (Å)	Au···H-X (deg)	H-X (Å)
B3LYP	HF	-19.96	2.16	180.0	0.98
TPSS		-23.24	2.06	180.0	1.00
MP2*		-19.89	2.15	180.0	0.96
MP2		-23.41	2.09	180.0	0.98
B3LYP	HCN	-16.52	2.36	180.0	1.11
TPSS		-18.93	2.22	180.0	1.13
MP2*		-19.55	2.25	180.0	1.11
MP2		-21.59	2.21	180.0	2.21
B3LYP	HCCH	-6.24	2.67	180.0	1.08
TPSS		-7.58	2.50	180.0	1.10
MP2*		-9.10	2.49	180.0	1.09
MP2		-10.30	2.44	180.0	1.09
B3LYP	H_2O	-11.63	2.40	161.9	0.99
TPSS		-13.15	2.29	165.1	1.01
MP2*		-12.97	2.37	161.7	0.98
MP2		-15.09	2.30	162.1	0.99
B3LYP	NH_3	-6.03	2.69	161.8	1.03
TPSS		-7.07	2.53	164.1	1.04
MP2*		-7.63	2.58	163.9	1.03
MP2		-8.86	2.51	162.9	1.03
B3LYP	CH_4	-1.18	3.22	179.9	1.09
TPSS		-1.65	3.04	180.0	1.10
MP2*		-2.47	2.93	180.0	1.09
MP2		-2.93	2.89	180.0	1.09

Table S2 – The E_{INT} values in kcal/mol, Au-CH_3 and H-X bond lengths and intermolecular distances in Å and bonding angles (°) of DMA H-Bonded to HF, HCN, HCCH, H_2O, NH_3 and CH_4.

Method	H-Donor	E_{INT} (kcal/mol)	Au-CH_3 (Å)	*d*(Au···H) (Å)	Au···H-X (°)	H-X (Å)
B3LYP	HF	-15.32	2.117	2.205	179.9	0.960
TPSS		-17.34	2.111	2.124	179.9	0.979
MP2*		-14.58	2.060	2.260	175.2	0.945
MP2		-16.00	2.061	2.222	174.4	0.954
B3LYP	HCN	-13.57	2.115	2.437	174.1	1.094
TPSS		-14.79	2.110	2.299	177.4	1.111
MP2*		-15.95	2.065	2.407	173.4	1.090
MP2		-16.17	2.065	2.388	173.5	1.092
B3LYP	HCCH	-5.05	2.717	2.117	174.2	1.077
TPSS		-5.76	2.580	2.111	176.2	1.086
MP2*		-6.99	2.611	2.062	173.2	1.078
MP2		-7.48	2.580	2.063	173.5	1.079
B3LYP	H_2O	-9.50	2.123	2.510	154.7	0.977
TPSS		-10.48	2.116	2.374	159.5	0.992
MP2*		-10.51	2.063	2.529	149.7	0.971

MP2		-11.52	2.064	2.468	151.3	0.976
B3LYP	NH_3	-4.81	2.120	2.729	160.0	1.023
TPSS		-5.45	2.112	2.596	162.4	1.033
MP2*		-4.61	2.061	2.677	160.1	1.021
MP2		-6.89	2.062	2.621	158.6	1.023
B3LYP	CH_4	-0.90	2.119	3.184	179.5	1.089
TPSS		-1.21	2.111	3.087	179.2	1.094
MP2*		-2.05	2.060	2.983	178.8	1.088
MP2		-2.40	2.061	2.915	179.2	1.089

Table S3 – E_{INT} values in kcal/mol for Au^- and DMA H-Bonded to HF, HCN, HCCH, H_2O, NH_3 and CH_4 optimised at the B3LYP/ aug-cc-pVTZ-pp level of theory in H_2O modelled as a continuum solvent.

H-Donor	E_{INT} (kcal/mol) with Au^-	E_{INT} (kcal/mol) with DMA
HF	-12.34	-8.02
HCN	-3.88	-2.50
H_2O	-5.08	-2.93
HCCH	-1.88	-0.81
NH_3	-2.04	-0.79
CH_4	-0.83	-0.03

Table S4 - The interaction energy (E_{INT}), intermolecular distance (M···H and H···CH_3) and H-F bond length in Å as comparison of M = Au(I), Cu(I) and Ag(I) dimethyl analogues at the MP2/aug-cc-pVTZ-pp level of theory.

	E_{INT} (kcal/mol)	*d*(M···H) (Å)	*d*(H···CH_3) (Å)	H-F (Å)
$[(Me)_2\text{-Au(I)}]^-$ ··H-F	-16.00	2.222	2.548	0.954
$[(Me)_2\text{-Ag(I)}]^-$···H-F	-15.66	2.413	2.070	0.952
$[(Me)_2\text{-Cu(I)}]^-$· ·H-F	-15.76	2.282	2.097	0.953

Table S5 – The interaction energy and three geometrical parameters of Au^- and DMA H-Bonded to HF when switching off relativistic effects.

Au^-.HF	E_{INT} (kcal/mol)	*d*(Au···H) (Å)	*d*(H···CH_3) (Å)	H-F (Å)
B3LYP/ ECP60MHF	-15.1	2.50		0.96
MP2/ ECP60MHF	-16.2	2.44		0.95
BP86-D3/TZP no ZORA	-17.3	2.33		0.99
DMA.HF				
B3LYP	-15.9	2.55	2.00	0.961
MP2	-15.2	2.54	2.06	0.951
BP86-D3/TZP no ZORA	-19.9	2.36	1.94	0.99

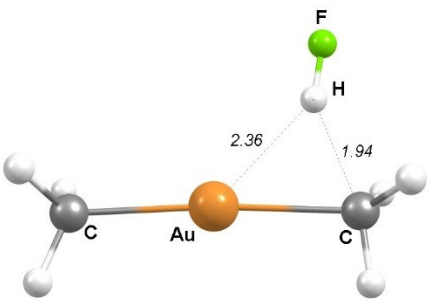

Figure S1 – Optimised geometry of the $[Me_2Au]^-$···HF adduct obtained at the BP86-D3 level of theory without ZORA.

S3. AIM and NCI parameters

Table S6 – Defined ranges for electron density [$\rho_b\ (ea_0^{-3})$], the Laplacian of the electron density [$\nabla^2(\rho_b)\ (ea_0^{-5})$] and the total electronic energy density [H_b (au)] for vdW, H-Bond and charge transfer in hypervalent trigonal bipyramidal adducts (CT-TBP) type interactions extracted from Nakanishi *et al*.[1]

Interaction type	$\rho_b\ (ea_0^{-3})$	$\nabla^2(\rho_b)\ (ea_0^{-5})$	H_b (au)
vdW	$0.00 < \rho_b < 0.01$	$0.00 < \nabla^2(\rho_b) < 0.04$	$0.00 < H_b < 0.002$
HB	$0.01 < \rho_b < 0.04$	$0.04 < \nabla^2(\rho_b) < 0.12$	$-0.004 < H_b < 0.002$
CT-TBP	$0.03 < \rho_b < 0.12$	$-0.01 < \nabla^2(\rho_b) < 0.1$	$-0.06 < H_b < -0.003$

Table S7 – The E_{INT} values in kcal/mol, the Au···H distances (Å), the electron density [$\rho_b\ (ea_0^{-3})$], the Laplacian of the electron density [$\nabla^2(\rho_b)\ (ea_0^{-5})$] and the total electronic energy density [H_b (au)] of six optimised H-Bonded Au^- adducts at the MP2/aug-cc-pVTZ-pp level of theory.

H-Donor	E_{INT} (kcal/mol)	Au···H (Å)	$\rho_b\ (ea_0^{-3})$	$\nabla^2(\rho_b)\ (ea_0^{-5})$	H_b (au)
HF	-23.41	2.09	0.039	0.043	-0.0117
HCN	-21.59	2.21	0.031	0.057	-0.0055
HCCH	-10.30	2.44	0.019	0.045	-0.0008
H_2O	-15.09	2.30	0.025	0.052	-0.0031
NH_3	-8.86	2.51	0.017	0.041	-0.0003
CH_4	-2.93	2.89	0.009	0.022	0.0005

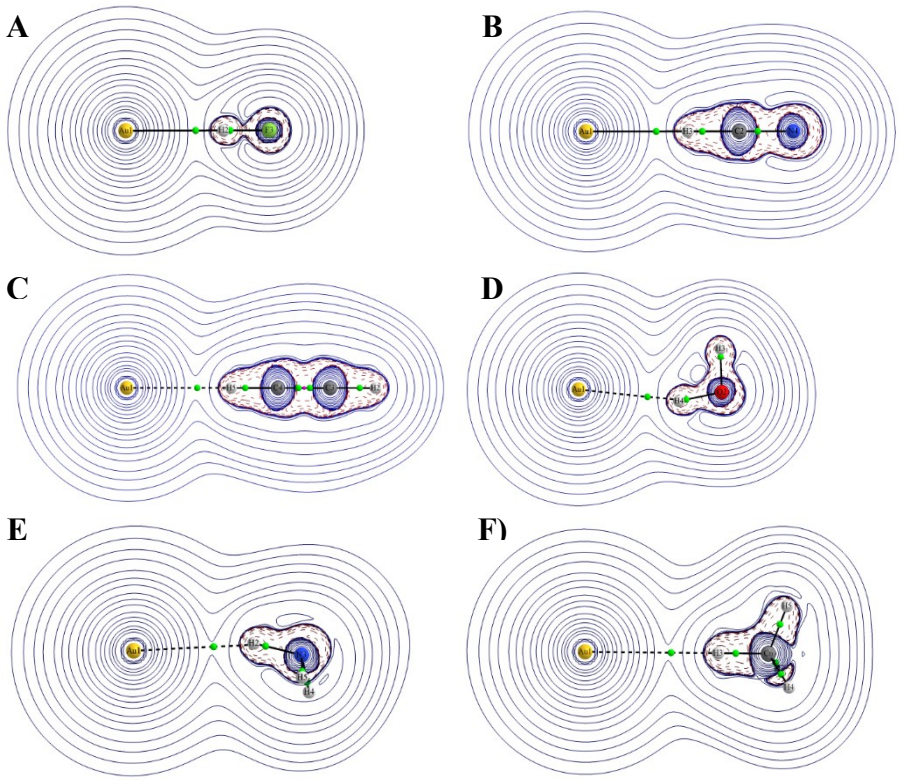

Figure S2 – Two dimensional contour plots for the $\nabla^2(\rho_b)$ of the H-Bonded optimised geometries in the gas phase of the auride anion with A) HF B) HCN C) HCCH D) H_2O E) NH_3 F) CH_4 at the MP2/aug-cc-pVTZ level of theory. The BCPs are shown as green spheres with the atomic interaction lines represented by the solid and dotted lines.

A)

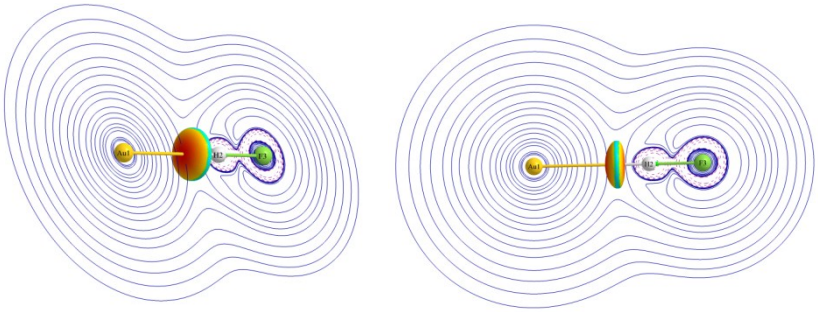

$Au^{-}\cdots HF$

Legend	$\lambda_2*\rho$ (au)
Red	-0.04794
Blue	0.02728

B)

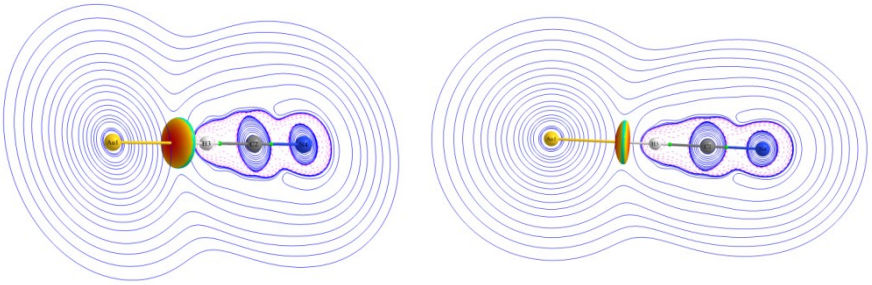

$Au^{-}\cdots HCN$

Legend	$\lambda_2*\rho$ (au)
Red	-0.03676
Blue	0.02153

C)

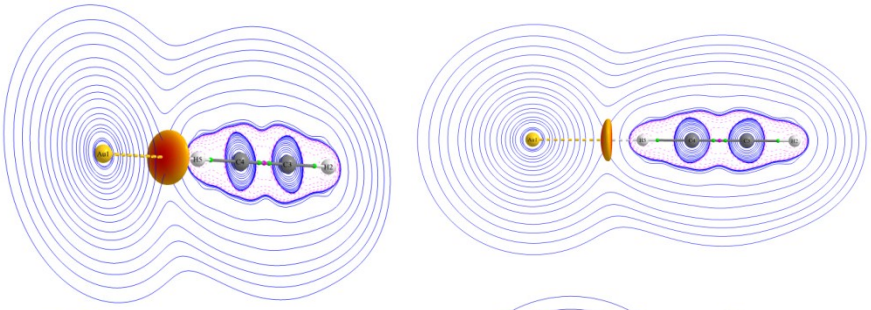

$Au^{-}\cdots HCCH$

Legend	$\lambda_2*\rho$ (au)
Red	-0.02095
Blue	-0.01347

D)

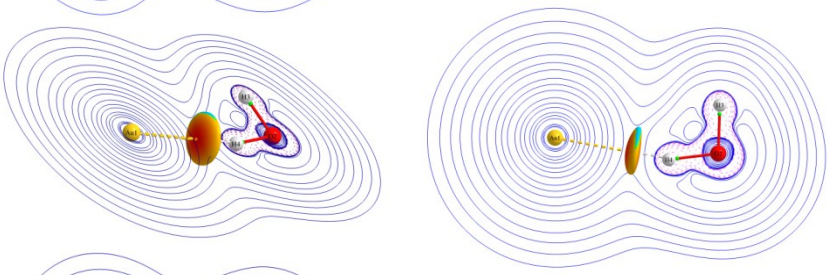

$Au^{-}\cdots H_2O$

Legend	$\lambda_2*\rho$ (au)
Red	-0.02835
Blue	0.01785

E)

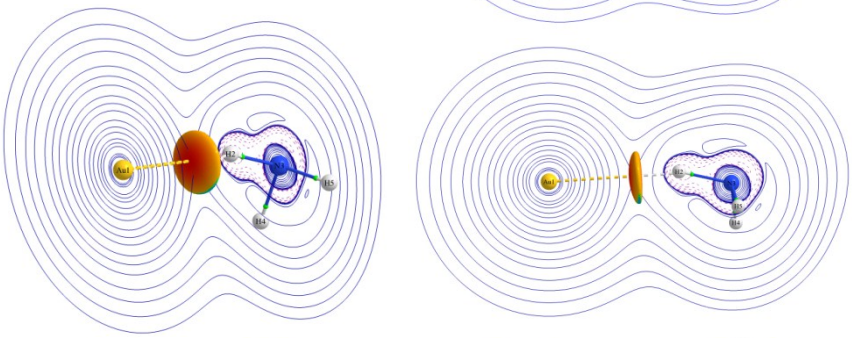

$Au^{-}\cdots NH_3$

Legend	$\lambda_2*\rho$ (au)
Red	-0.01828
Blue	0.01166

F)

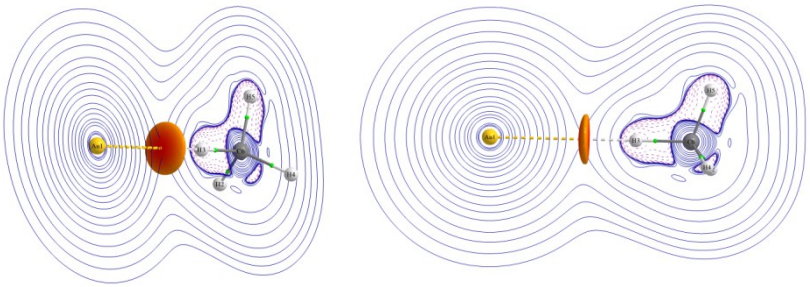

$Au^{-}\cdots CH_4$

Legend	$\lambda_2*\rho$ (au)
Red	-0.00917
Blue	-0.00655

Figure S3 – NCI plots and two dimensional contour plots of the $\nabla^2(\rho_b)$ calculated for the auride anion H-Bonded to six H-Bond donors; A) HF, B) HCN, C) HCCH, D) H_2O, E) NH_3 and F) CH_4. The $\lambda_2*\rho$ (au) values are indicated in the tables next to each image. Red indicates the Minimum value, yellow indicates values less than zero, green indicates zero and blue indicating the maximum and cyan greater than zero.

Table S8 – The E_{INT} values, the Au···H distance in Å, the electron density [$\rho_b\ (ea_0^{-3})$], the Laplacian [$\nabla^2(\rho_b)\ (ea_0^{-5})$] and the total electronic energy density [H_b (au)] of the optimised geometries of the DMA adducts at the MP2/aug-cc-pVTZ-pp level of theory.

H-Bond donor	E_{INT} (kcal/mol)	d(Au···H) (Å)	$\rho_b\ (ea_0^{-3})$	$\nabla^2(\rho_b)\ (ea_0^{-5})$	H_b (au)
HF	-16.00	2.22	0.028	0.048	-0.0052
HCN	-16.17	2.39	0.021	0.051	-0.0012
HCCH	-7.48	2.06	0.014	0.039	0.0004
H_2O	-11.52	2.47	0.017	0.046	-0.0003
NH_3	-6.89	2.62	0.013	0.037	0.0005
CH_4	-2.40	2.92	0.008	0.022	0.0007

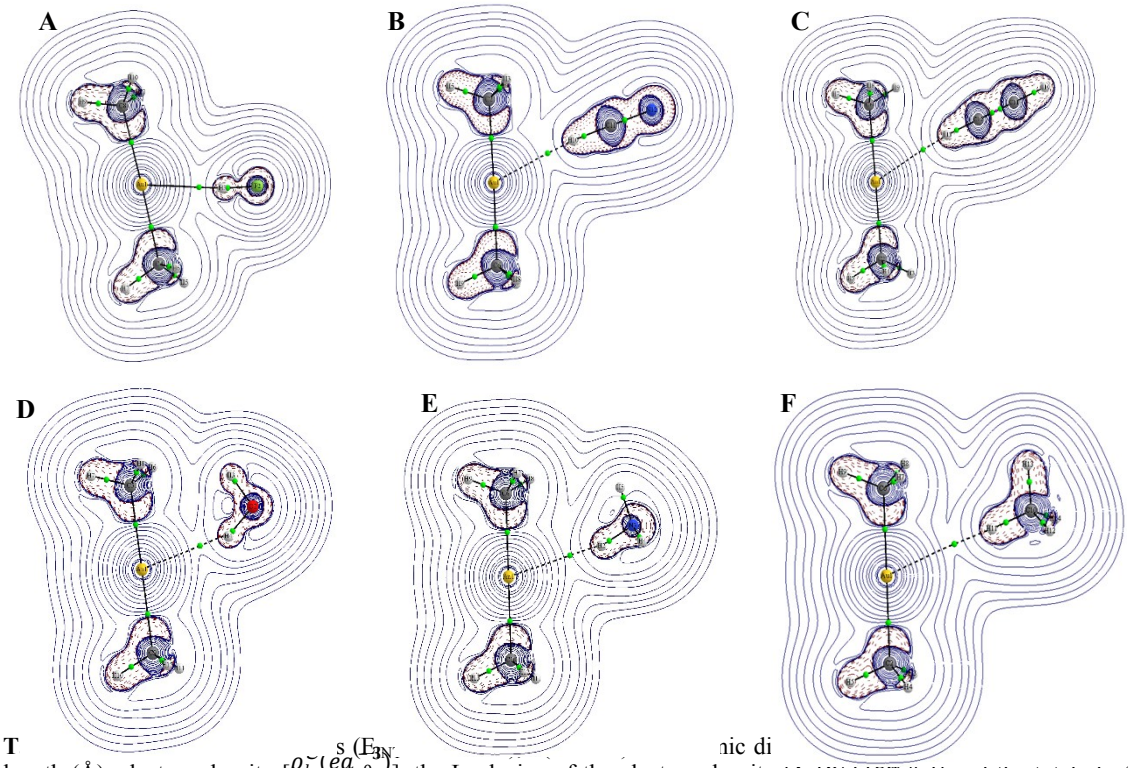

T s (E_{IN} nic di bond length (Å), electron density [$\rho_b(ea_0^{-3})$], the Laplacian of the electron density [$\nabla^2(\rho_b)\ (ea_0^{-5})$] and the total electronic energy density [H_b (au)] of the Au···HF and [Me-Au]···HF adducts at the MP2 level of theory with relativistic effe

Figure S3 – Molecular graphs and two dimensional contour plots of $\nabla^2(\rho_b)$ of the optimised geometries of the DMA Au(I) anionic complex H-Bonded to A) HF B) HCN C) HCCH D) H_2O E) NH_3 F) CH_4 at the MP2/aug-cc-pVTZ level of theory

Au^-	0.018	0.029	-0.0017
DMA	0.024[a]	0.048[a]	-0.0026[a]

[a] Properties of the C···H interaction

S4. EDA analysis

Table S10 – EDA results at the BP86-D3/TZP level of theory in kcal/mol for adducts with Au^- and DMA.

	Au^-.HF	**Au^-.HCN**	**Au^-.H_2O**	**Au^-.HCCH**	**Au^-.NH_3**	**Au^-.CH_4**
E_{int}	-23.01	-20.42	-14.33	-9.51	-8.67	-2.87
ΔE_{elstat}	-23.63 (55.3%)	-24.73 (56.5%)	-15.68 (61.4%)	-11.6 (50.7%)	-11.23 (58.2%)	-3.17 (40.3%)
ΔE_{Pauli}	19.72	23.33	11.19	13.37	10.63	5
ΔE_{orb}	-18.27 (42.7%)	-17.93 (41.0%)	-8.37 (32.8%)	-10.03 (43.9%)	-6.45 (33.4%)	-3.43 (43.6%)
ΔE_{disp}	-0.84 (2.0%)	-1.08 (2.5%)	-1.47 (5.8%)	-1.24 (5.4%)	-1.62 (8.4%)	-1.27 (16.1%)
	DMA.HF	**DMA.HCN**	**DMA.H_2O**	**DMA.HCCH**	**DMA.NH_3**	**DMA.CH_4**
E_{int}	-17.97	-17.18	-12.74	-8.34	-7.95	-2.98
ΔE_{elstat}	-16.32 (53.8%)	-17.29 (56.5%)	-12.09 (58.8%)	-7.51 (45.2%)	-8.03 (52.7%)	-2.2 (31.4%)
ΔE_{Pauli}	12.35	13.43	7.82	8.27	7.31	4.02
ΔE_{orb}	-12.16 (40.1%)	-10.88 (35.5%)	-5.78 (28.1%)	-6.64 (40.0%)	-4.32 (28.3%)	-2.53 (36.1%)
ΔE_{disp}	-1.84 (6.1%)	-2.44 (8.0%)	-2.68 (13.0%)	-2.46 (14.8%)	-2.9 (19.0%)	-2.27 (32.4%)

S5. Effect of adduct formation on H-X bond

Table S11 - Elongation of the H-X bond (Å) upon H-bond formation with Au^- and DMA at the MP2/aug-cc-pVTZ level of theory.

	Au^-	DMA
	ΔR (Å)	ΔR (Å)
HF	0.056	0.030
HCN	0.055	0.028
HCCH	0.030	0.017
H_2O	0.031	0.015
NH_3	0.019	0.011
CH_4	0.005	0.003

Table S12 Unscaled calculated H–X stretching frequencies (cm^{-1}) for HF, HCN, HCCH, H_2O, NH_3 and CH_4 adducts with Au^- and $[Me_2Au]^-$ and theoretical and experimental IR frequencies for the isolated H-bond donors at the MP2/aug-cc-pVTZ-pp level of theory.

	$Au^-\cdots$H-X	DMA$\cdots$H-X	H-X	Exp.
HF	2971.6	3444.7	4122.9	3953[2]
HCN	2682.9	3057.0	3465.7	3438.5[3]
HCCH	3026.7	3226.6	3431.6	3372[4]
H_2O	3289.7	3604.2	3948.0	3942[3]
NH_3	3274.2	3549.1	3649.9	3577[5]
CH_4	3147.4	3171.5	3204.7	3252[3]

References

1 W. Nakanishi, S. Hayashi, K. Narahara, *J. Phys. Chem. A*, 2008, **112**, 13593.

2. M. T. Bowers, G. I. Kerley and W. H. Flygare, *J Chem. Phys.*, 1966, **45**, 3399.

3. C. H. Choi and M. Kertesz, *J. Phys. Chem.*, 1996, **100**, 16530.

4. W. F. Murphy, W. Holzer and H. J. Bernstein, *Appl. Spectrosc.*, 1969, **23**, 211.

5. L. Fan and T. Ziegler, *J. Chem. Phys*., 1992, **96**, 9005.